J Nanostruct 11(2): 276-285, Spring 2021

RESEARCH PAPER

Mg-doped NiO Nanoparticles Decorated Multi-Walled Carbon Nanotube (MWCNT) Nanocomposite and their Biological Activities

Noor Q. Ali, Ali A. Taha , Duha S. Ahmed*

Applied Sciences Department, University of Technology, Baghdad 100001, Iraq

ARTICLE INFO

Article History:
Received 10 December 2020
Accepted 15 March 2021
Published 01 April 2021

Keywords:
Anticancer activity.
Carbon nanotubes (CNTs);
MCF-7 cell
Nickle oxide (NiO)
Sol-gel method;

ABSTRACT

Here we report a novel nanocomposite composed from Mg-doped NiO and Mg- doped\MWCNTs using a facile sol-gel method. The synthesized Mg-doped NiO and Mg- doped\MWCNTs nanocomposite was characterization by XRD diffraction Analysis (XRD), Energy dispersive X-ray spectroscopy (EDS), Fourier transform infrared spectroscopy (FTIR), Filed Emission scanning electron microscopy (FESEM), and UV-Vis spectrophotometer. The X- Ray analysis revealed that the formation of nanocomposites, which has a cubic phase and a high crystalline nature. The FE-SEM images confirmed the success of decoration the Mg- doped NiO on the surface of the treated MWCNTs through the emergence of spherical shapes over the cylindrical tubes. Conversely, optical measurements reveal that the energy gap value for the Mg- NiO and the Mg/NiO-MWCNTs nanocomposite are 3.28 eV and 2.82 eV, respectively. This indicates decreasing the zone between conduction band and valence band. Moreover, it found that Mg-doped NiO\MWCNTs nanocomposite showed high removal efficiency towards the lead element compared with the Mg-doped NiO. Also, MTT test was employed to study antitumor activity against MCF-7 and WRL68 cells. Our results showed that the Mg doped NiO-MWCNTs had cell viability of 66.7% and 71.9 % against MCF-7 and WRL68, respectively. In state of Mg- doped NiO sample was display cell viability of 70.2% and 71.9 % against MCF-7 and WRL68, respectively

How to cite this article
Ali N.Q., Taha A.A., Ahmed D.S. Mg-doped NiO Nanoparticles Decorated Multi-Walled Carbon Nanotube (MWCNT) Nanocomposite and their Biological Activities. J Nanostruct, 2021; 11(2): 276-285. DOI: 10.22052/JNS.2021.02.008

INTRODUCTION

Recently, nanotechnology has entered many areas of life, such as biomedicine, food, energy, electronics, textile, environment, solar cells, and hydrogen fuel cells [1]. Carbon is one of the most common elements found on the surface of the earth, and it appears in a variety of forms, namely, carbon nanotubes (CNTs) and graphene [2]. In state of Multi-Walled Carbon Nanotubes (MWCNTs), that concerned grate consideration due to the remarkable properties such as extremely light weight, high chemical and thermal stability, and high tensile strength, resistance to basic and acidic media. The MWCNTs also play an important role in preparing nanocomposites and treating water pollution [3-5]. The MWCNTs are produced from various methods including arc chemical vapor deposition (CVD) [6], hydrothermal processes [7], discharge [8], laser ablation [9], etc. To improve the performance of MWCNTs, the decorating them with metal oxides has been widely used due to good merits such as thermal

* *Corresponding Author Email: as.18.70@grad.uotechnology.edu.iq*

stability and, high mechanical strength. Moreover, the dopants of MWCNTs reduces the band gap, to produce an effective metal oxide nanoparticle in the ultraviolet and visible region [10]. Among the many metal oxides, nickel oxide (NiO) nanoparticle was used as dopant with MWCNTs to produce a more effective compound. The Multi-walled carbon nanotubes (MWCNTs) act as a dispersing agent that prevents NiO nanoparticles from accumulation, which result in increasing the surface area compared to pure NiO. NiO is a transition metal oxide has a cubic structure. It is also a p- type semiconductor material with stable band gap in range of 3.6-4.0 eV. Although most NiO is used as an antiferromagnetic insulator [11]. Moreover, NiO doped with elements like Zn, Mg, and Li etc. result in various charge transfer properties between the prepared material and the surrounding environment. The degree of metal dispersion on the particle surface and the homogenous of chemical structure of particle depend obviously on the doping methods and annealing temperature, which result to different morphology and properties [12].

Recently, the cancer cell is one of the most difficult diseases that the world has faced in recent years due to the increase in the number of cases up to 25 million annually in a year 2015. There are many common methods of treating cancer, such as radiotherapy, surgery, and chemotherapy [13]. MWCNTs work to make cancer drugs accumulate at the tumor site by enhanced penetration effect. Since CNT has high elasticity, good stability, and biocompatibility, it can easily penetrate biological barriers and destroy the contents of the cancer cells [14, 15].

This article includes the synthesis of NiO nanoparticles doped with Mg element as well as synthesis Mg-doped NiO\MWCNTs nanocomposite using sol-gel method. The structural, optical and morphological properties have been identified via characterization process represented by XRD, FTIR, EDX, FESEM and UV-Vis spectroscopy. The anticancer activity of the prepared nanostructures was determined by the studying cytotoxicity effect of Mg-doped NiO and Mg-doped\MWCNTs nanocomposite against breast cancer (MCF-7) and normal human cells (WRL68) utilizing MTT assay.

MATERIALS AND METHODS

Magnesium nitrate hexahydrate (Mg $(NO_3)_2.6H_2O$), nickel nitrate hexahydrate ($Ni(NO_3)_2.6H_2O$), ($Mg:NiO_2$ = 6% in mole ratio) and oleic acid ($C_{18}H_{34}O_2$) were bought from Sigma-Aldrich (USA). Multi-walled carbon nanotubes (MWCNTs, purity >95 wt%; diameter ~8-15nm; length ~10-50pm; Ash<1.5 wt%) were provided from Cheaptubes.com Grafton (USA). Each solution was prepared utilizing deionized water.

Treatment of MWCNTs

In this step, functionalized MWCNTs is formed by adding 0.5g of pristine -MWCNTs in a mixture of (95% H_2SO_4) and (65% HNO_3) with ratio 3:1 v\v to result several functional groups on treated F-MWCNTs. The mixture was sonication in ultrasonic bath for 30min at temperature 30°C to increase dispersion quality of functionalized MWCNTs (F-MWCNTs). Afterwards, the mixture was then diluted with 400ml of distilled water and washed several times by using vacuum filtered through micro membrane (0.22pm) made from cellulose nitrate to remove any impurities from functionalized -MWCNTs. Finally, the filtered samples products were dried in oven for 24h at 100°C to form functionalized MWCNTs samples.

Synthesis of Mg-doped NiO nanoparticles

In this step, Mg-doped NiO NPs was synthesized by sol-gel process. In state of doped NiO NPs, Magnesium nitrate hexahydrate (Mg $(NO_3)_2.6H_2O$) and Ethyl alcohol ($C_{18}H_{34}O_2$) were added as precursor. 3g of Mg $(NO_3)_2.6H_2O$ was added to 50 ml of ethyl alcohol and stirred for 1h until the mixture dissolve completely. Also, 5g of Ni $(NO_3)_2.6H_2O$ was dissolve in 50ml of ethylalcohol. The prepared solutions was mixed and stirred together on magnetic stirring for 1 h at temperature 60°C. Afterwards, the oleic acid was added to the resulting solution slowly with constant stirred resulting thick gel. Then the resulted samples of Mg-doped NiO NPs was dried in oven at 100°C for 24h and followed by calcined for 4h at 600°C.

Synthesis of Mg-doped NiO/MWCNTs Nanocomposite

Mg-doped NiO\MWCNTs nanocomposite was prepared by using 1:1 weight ratio of Mg-doped NiO and functionalized MWCNTs. Since, 0.3g of Mg-doped NiO NPs was dissolved in 50ml of deionized water with 0.3g of functionalized MWCNTs. The mixture was sonication for 15min and stirred for 30min at 80°C. Subsequently, added

2ml of NaOH was a surfactant to the mixture and stirred for another 2h to adjust the pH value and sol- was produced. After that, the resulted mixture was washed and filtered with absolute ethanol and deionized water several times to remove any impurities. The prepared gel was dried at 120°C for 3h and calcinated for 2h at 450°C in oven at atmospheric pressure to obtain dry powder of Mg-doped NiO\MWCNTs nanocomposite.

Characterization

The crystal structure and crystallite size of the prepared Mg-doped NiO and Mg-doped NiO\MWCNT nanocomposite were identified by X-ray spectrum (XRD-6000, Shimadzu) with Cu Ka radiation source (wavelength of 1.54056 A) at diffraction angle (29) from 20° to 80°. The chemical composition and functional groups was determined through the FT-IR technique (8400S, Shimadzu) in the range 400-4000 cm^{-1}. Also, the morphology of the prepared samples can be identified by field emission scanning electron microscopy (FESEM) (Hitachi Type S-4160. The optical band gap of Mg-doped NiO NPs and Mg-doped NiO\MWCNTs nanocomposite were determined by UV.vis spectroscopy (1800, Shimadzu, Kyoto, Japan).

MTT Assay of Determination of antitumor activity

The MTT assay has been used to assess the cytotoxic effect of prepared Mg-doped NiO and Mg-doped NiO\MWCNT nanocomposite on different concentrations of tumor cell lines (MCF-7) and normal cell line (WRL 68) that isolated from *L. camara* crude extracts. These cells were grown in RPMI-1640 medium at 37°C with 5% CO_2 in 96 -well flat bottom culture plates at density $1*10^4$ cells /ml for 48 h. The cells were treated, in duplicate, with the concentrations of 12.5-400 pg/ml of Mg-doped NiO and Mg-doped NiO\MWCNTs nanocomposite, respectively incubated for 24 h to determine the toxicity against examined cell lines.

10pl of prepared MTT solution was addition to each well. Moreover, the plates were incubation at 37°C, 5%CO_2 for 4h. Then, removing the media gradually and 100 pl of solubility solution were added per each well doe 5 min. The absorbance of samples was measured by using the ELISA reader at wavelength 575nm. The resulted data of optical density was submitted to statistical analysis in order to calculate the concentration of required nanostructure to result 50% limitation in cell viability for each cell line. The cytotoxicity percentage was determined by the equation (1):

Growth inhibition rate % (G.I) = A-B\A x100 **(1)**

RESULTS AND DISCUSSION

Structural Measurements

Fig. 1 represents the XRD patterns of Mg-doped

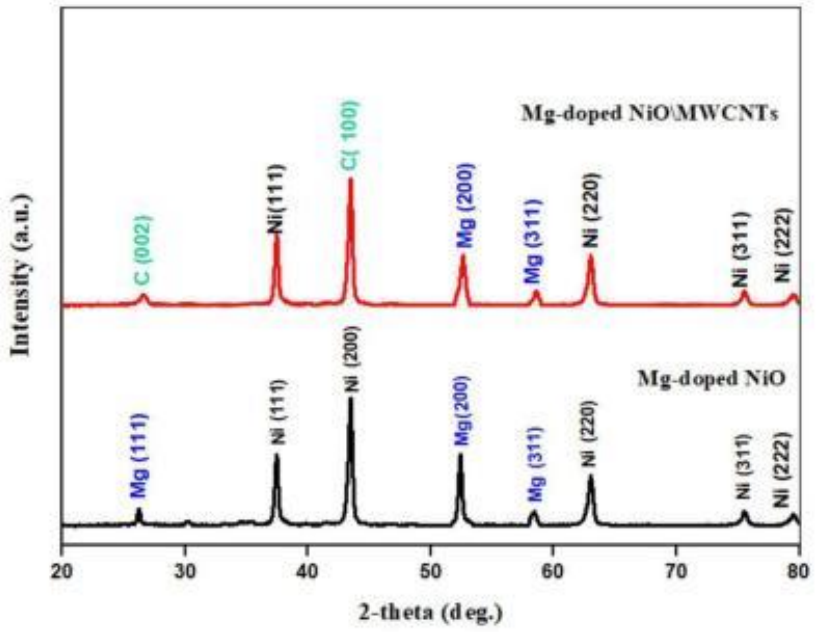

Fig. 1. XRD patterns of Mg-doped NiO and Mg-doped NiO/MWCNT nanocomposites

Table 1. XRD analyses for Mg-doped NiO and Mg-doped NiO\MWCNTs NPs

Sample	phase	20	Plane (hkl)	FWHM	Crystalline Size D (nm)	d (A)
Mg doped-NiO	Mg	26.23	(111)	0.2952	53.33	3.39685
	Ni	37.45	(111)	0.2460		2.10114
	Ni	43.48	(200)	0.2460		2.08117
	Ni	52.24	(220)	0.2460		1.75736
	Mg	58.42	(311)	0.3425		1.55965
Mg doped-NiO\MWCNTs	C	26.62	111	0.98	25.43	3.42
Sample	phase	20	Plane (hkl)	FWHM	Crystalline Size D (nm)	d (A)
Mg doped-NiO	Mg	26.23	(111)	0.2952	53.33	3.39685
	Ni	37.45	(111)	0.2460		2.10114
	Ni	43.48	(200)	0.2460		2.08117
	Ni	52.24	(220)	0.2460		1.75736
	Mg	58.42	(311)	0.3425		1.55965
Mg doped-NiO\MWCNTs	C	26.62	111	0.98	25.43	3.42

NiO and Mg-doped NiO\MWCNTs nanocomposite, respectively. The XRD pattern of Mg-doped NiO (black line) displayed diffraction peaks at 29 = 37.33°, 43.27°, 62.43°, 75.47°, and 79.42° are corresponding to the hkl planes of (111), (200), (220), (311), and (222), respectively. This confirms the formation of cubic structure of NiO NPs. As well as, the diffraction peaks at 29 =26.3°, 52,29 ° and58.38°, are corresponding to the hkl planes of (111), (200) and (311), respectively which are related to the formation the Mg-NiO compound [16]. Moreover, the XRD pattern of Mg-doped NiO\ MWCNTs nanocomposite (red line) are displayed different groups appears in patterns. The peaks at 29 = 37.41°, 63.02°, 75.52°, and 79.25° are attributed to the hkl planes of (111), (220), (311), and (222) and matches well with NiO structure. These patterns indicate the cubic structure of NiO (JCPDS Card No: 78-0643) [17]. As shown in Fig. 1, there are a diffraction peaks at 29 =26.37°, 52,29 ° and 58.38°, are corresponding to the hkl planes of (111), (200) and (311), respectively which are related to the formation the Mg-NiO nanocomposite as shown in previous results before addition MWCNTs [16]. Besides, the XRD pattern of Mg-doped NiO\MWCNT nanocomposite reveals tow diffraction peaks at 29 = 26.6° of (002) and high intensity at 29 = 43.46° of (100) crystal plane related to the graphitic structure through the acid treatment of MWCNTs related to JCPDS no. 01- 0646) [4, 17]. The average crystal size calculated using Debye-Scherer's equation of Mg-NiO and Mg-doped NiO\MWCNT nanocomposites are about 53.33nm and 25.43 nm, respectively as shown in Table 1. These results, improve the success of combination Mg-NiO with F-MWCNTs as composite without any damage in the structure by using Sol-gel method.

The results of FTIR spectra of Mg-doped NiO and Mg-NiO\MWCNTs nanocomposites in a range of 400-4000 cm^{-1} were represented in Fig. 2. FTIR spectrum of prepared Mg-doped NiO sample (green line) reveals the appearance absorption peaks located at 2925.01cm^{-1} is due to the C-H stretching vibration due to the residual amorphous carbon species in oleic acid. The absorption peaks appear around 1502cm^{-1} and 1458.99cm^{-1}, are related to bending mode of H-O- H and carbocyclic groups of NiO. Finally, weak absorption peaks at 722.08$cm^{-1}$and 504.16cm^{-1} confirm the metal-oxide formation between (Ni-O and Mg-O) which reveal the formation Mg- doped NiO NPs [18-21]. In state of Mg-doped NiO\MWCNTs nanocomposites (red line), it was observed the appearance of a

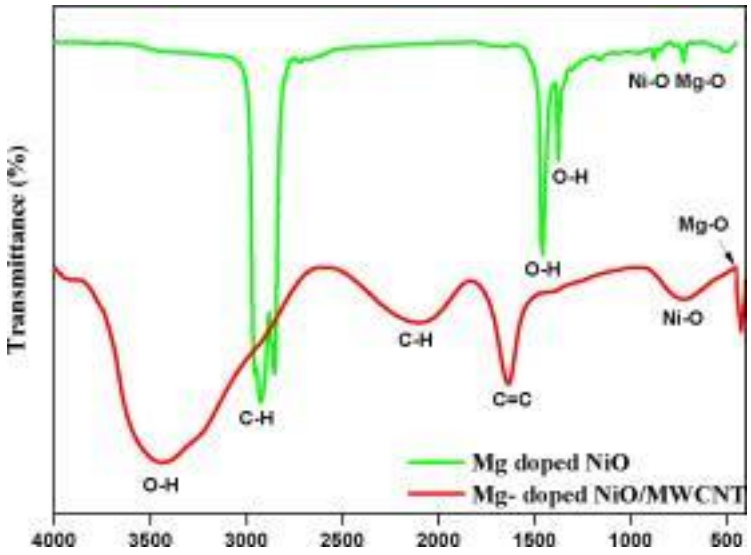

Fig. 2. FTIR analysis of Mg-doped NiO and Mg-doped NiO\MWCNTs nanocomposite

wide peaks in the range (3435-3437) cm^{-1} due to the stretching vibration of hydroxyl groups (O-H). The absorption peaks around (2078-2109) cm^{-1} are appeared related to the stretching vibration of C-H bond of CH_2 and CH_3 groups represented in residual amorphous carbon species in the FTIR spectra. Conversely, the absorption peaks around 1638 cm^{-1} are due to the stretching vibration of the carbon molecules (C=C) in carbon backbone structure of MWCNTs. Finally, the weak absorption peaks around (709-711) cm^{-1} are related to the stretching vibration of the Ni-O bond in Mg-doped NiO. The band at 419cm^{-1} is corresponding to the stretching vibrational mode of Mg-O bond [20, 22, 23]. The results of FTIR reveal that nanoparticles are prepared and attach to treated MWCNTs and formation new bonds due to the interaction between MWCNTs and Mg-doped NiO.

Morphological Measurements

Fig. 3a,b represents the FE-SEM images of Mg-doped NiO and Mg-NiO\MWCNTs nanocomposites, respectively. It is observed in Fig. 3 a,b, that Mg-doped NiO displays a smooth surface covered with particles of spherical shapes of Mg and asymmetric sizes distributed over the surface [24]. FESEM images of the nanocomposite Mg-doped NiO/MWCNTs are shown in Fig. 3c,d with different magnifications. It can be seen that the Mg-doped NiO nanoparticles specially attached to the surfaces of treated MWCNTs rather than to other regions without MWCNTs. The FESEM analysis demonstrates the light spots which relate to Mg- doped NiO nanoparticles decorated the tubes. As display in these Figures, the side walls of MWCNTs are evenly decorated with Mg-doped NiO nanoparticles and there are NPs aggregates on the wall of MWCNTs which are so dense and not uniform, that it is hardly to see the hollow cavity of the tubes, which may result from the application of heat for a long time [28]. The particle size mean of Mg-doped NiO and Mg-doped NiO\MWCNT nanocomposite are about 78.26 nm and 35.02 nm., respectively. This confirms the Mg-doped NiO nanoparticles and its heterogeneous dispersed on the surface of the F-MWCNTs. The results obtained from the FESEM analysis are similar to a study prepared by Saravanakkumar et al. [25], Karnaukhov et al. [26], and Mustafa et al. [27].

Besides, the EDS spectrum of Mg-doped NiO displays the appearance of oxygen, nickel and magnesium elements, and this indicates that Mg is successfully doped in NiO sites during the chemical reaction formation Mg-NiO as shown in Fig. 4 a. We observe a clear increase in the weight ratio of Mg from 2.78% to 3.48% at high concentration of Mg (except at 4% Mg). In contrast, EDS analysis for Mg-doped NiO\MWCNTs nanocomposite is demonstrate in Fig. 4 b.

Optical Measurements

The optical properties of the prepared colloidal solutions can be identified via UV-Vis spectroscopy

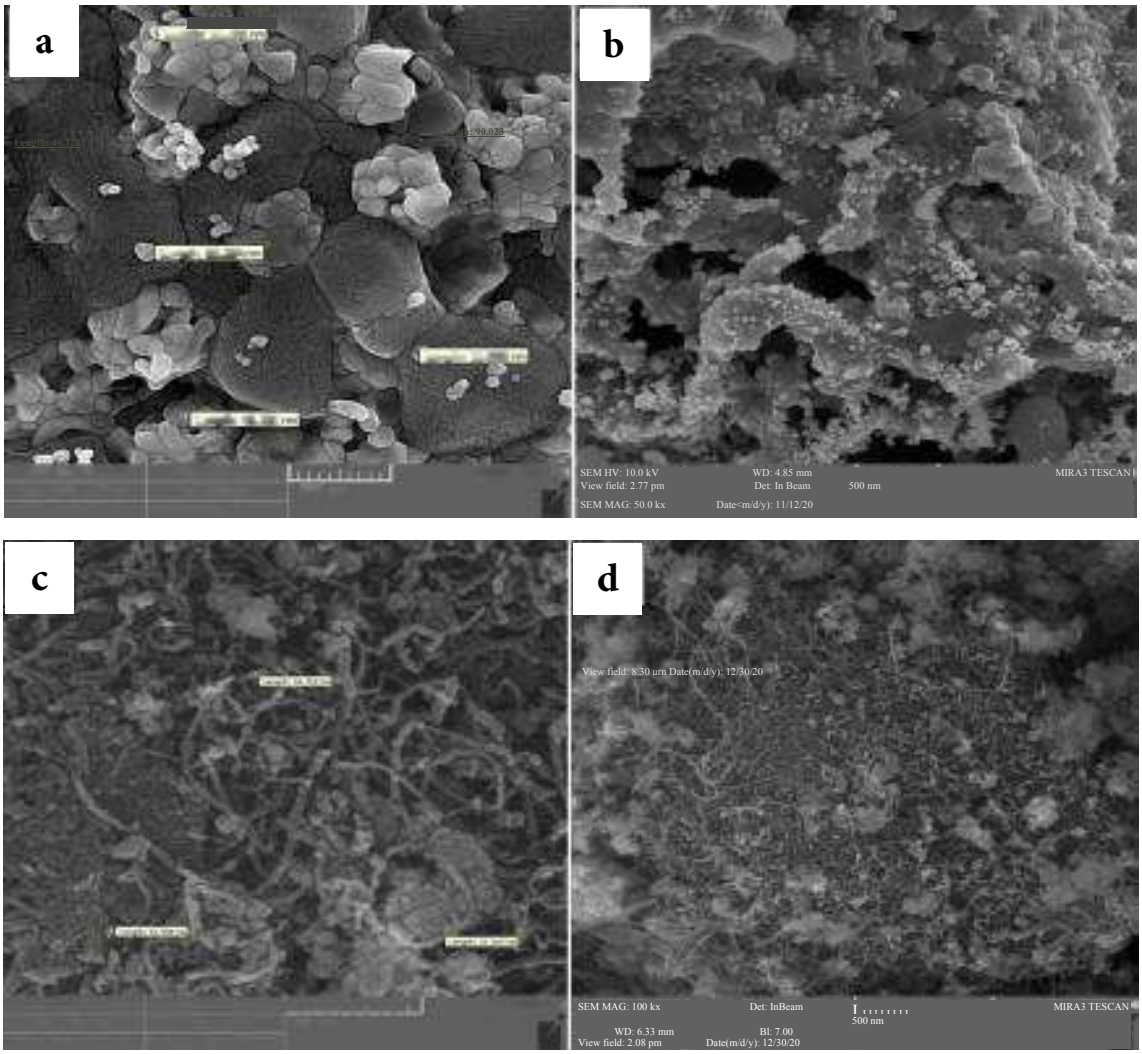

Fig. 3. FESEM images of (a, b) Mg-doped NiO and (c, d) Mg-doped NiO/MWCNTs nanocomposite.

in the wavelength range of 200-800 nm, as shown in Fig. 5. The absorption spectrum of Mg-doped NiO shows a broad absorption peak at wavelength of 265 nm. In contrast, the UV-Vis spectra of the Mg-doped NiO\MWCNTs nanocomposite display a shift towards the higher wavelength (red shift) at absorption peak at 361 nm with an apparent higher band intensity [28, 29]. In state of measurement the optical band gap energy (E_g) for all samples can be calculated by Tauc's equation [30]:

$$(ahu)^2 = A\ (hu\text{-}E_g) \qquad (2)$$

Where hv is the photon energy, E_g is the optical band gap energy, and A is a constant. Fig. 6 displays the energy band gap spectrum of Mg-doped NiO and Mg- doped NiO\MWCNTs nanocomposite. Where the energy band gap is estimated by plotting (ahu) against the photon energy (hu) and a linear extrapolating at the absorption edge toward the x-axis. It is observed that the energy gap value (E_g) of the Mg-doped NiO up to 3.28 eV. In contrast, the band gap energy value of the nanocomposite up to 2.82 eV. An obvious decrease in the E_g was observed, which related to the capability of the treated MWCNTs to become as photogenertaed of electron assepters and SPR (surface plasmon resonace) [31].

Biological Treatments

Antitumor activity of Mg-doped NiO and Mg-doped NiO/MWCNTs nanocomposites was evaluated against MCF-7 as tumor cell and WRL68 as normal cell lines. The MTT assay was used to

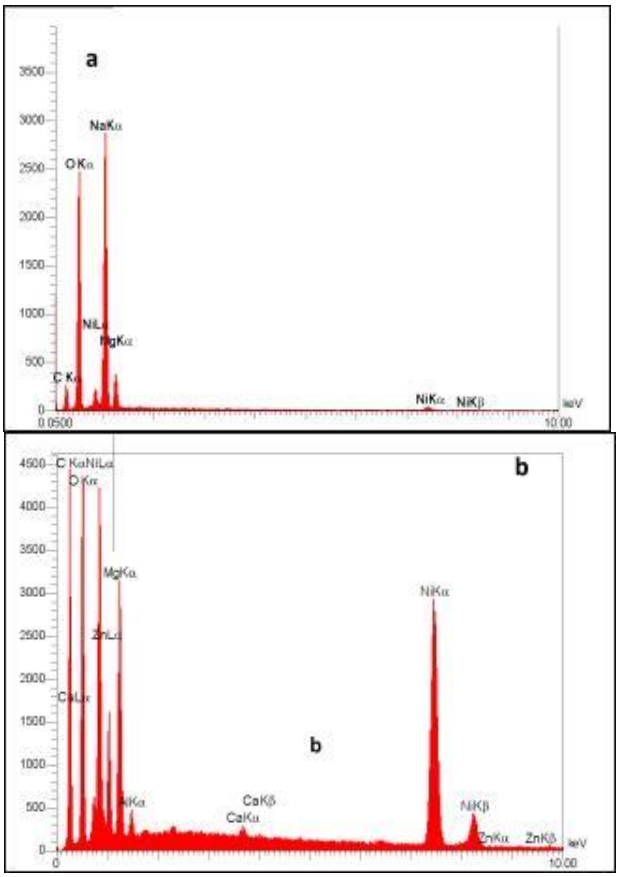

Fig. 4. The EDS analysis of a) Mg-doped NiO and b) Mg-doped NiO/MWCNTs nanocomposite The EDS analysis confirms the appearance of nickel and magnesium components in the hybrid sample beside to carbon and oxygen. These results indicate the success of forming the Mg-doped NiO\MWCNT nanocomposite. Moreover, the appearance of weak peaks in the EDS spectrum were due to the presence of small content of contaminants such as aluminum (Al, 3.01%), calcium (Ca, 1.21%), and zinc (Zn, 5.26 %) as shown in Table2[25].

Table 2. The EDS analysis of a) Mg-doped NiO and b) Mg-doped NiO/MWCNTs nanocomposite

Sample	C	O	Ni	Mg	Na	Ca	Zn
	W%	W%	W%	W%	W%	W%	W%
Mg- NiO	17.79	50.05	2.33	3.48	26.35	--	-—
Mg-NiO\MWCNTs	20.00	27.34	18.07	16.12	-—	1.21	5.26

determine cell viability of different concentrations (25, 50, 200 and 400) pg/ml of synthesized Mg-doped NiO and Mg-doped NiO/MWCNTs nanocomposites against MCF-7 tumor cell and WRL68 normal cell , respectively after incubated at 37 °C for 24 h in the presence of 5% CO_2 as shown in Fig. 7 (a,b). As shown in the Figure, the higher concentration (400 pg/ml) of Mg-doped NiO and Mg-doped NiO/MWCNTs nanocomposites, respectively resulted in high toxicity against the examined cells. Moreover, the cell viability reached to (70.2%-71.9%) in the presence of Mg-doped NiO, while it is about (66.7%- 71.9%) in the presence of Mg-doped NiO/MWCNTs nanocomposites against MCF-7 and WRL-68 cell lines, respectively, as shown in Fig. 7 a,b. Based on these results, the tumor can be treated either physical effect using radiation and hyperthermia thereby, or chemical effect by intracellular entry of doped nanoparticles Mg-doped NiO and Mg-doped

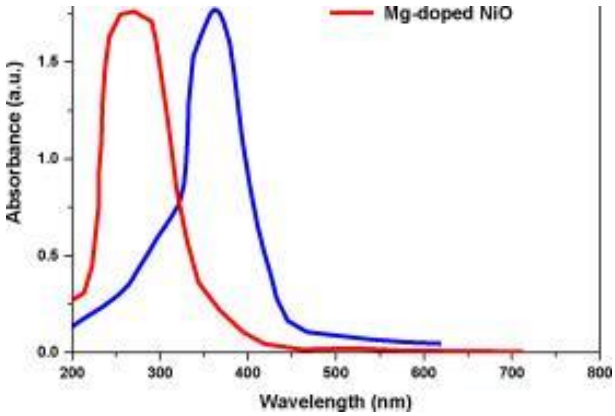

Fig. 5. The Optical absorption spectra of Mg-doped NiO and Mg-doped NiO/MWCNTs nanocomposite

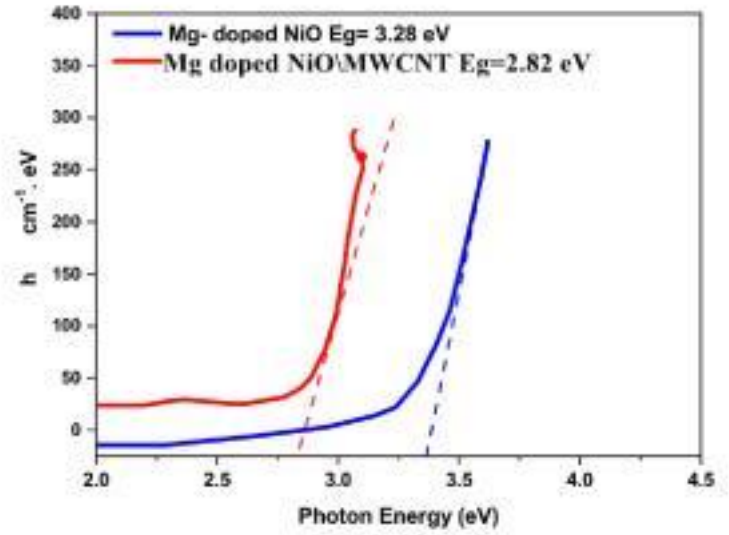

Fig. 6. Plot of variation of $(ahv)^2$ vs. photon energy of Mg-doped NiO and Mg-doped NiO/MWCNTs nanocomposite

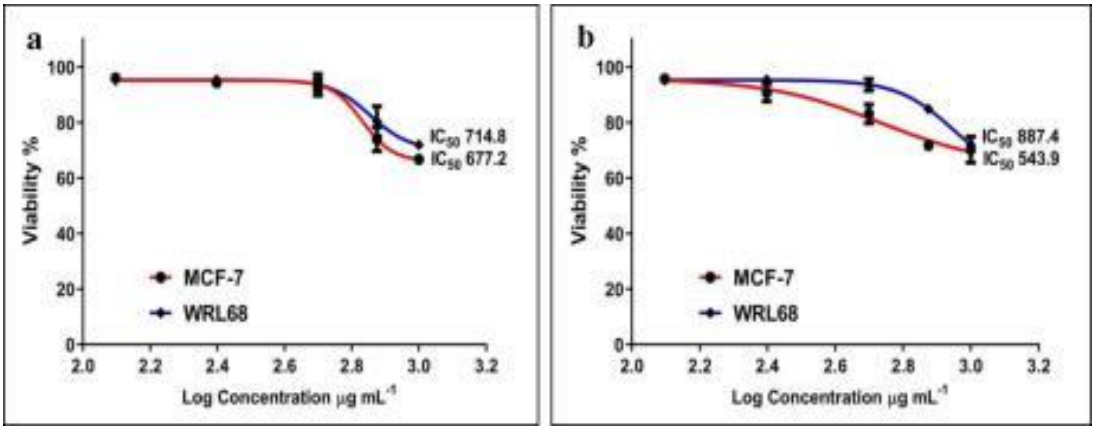

Fig. 7. Viability percentage of cell lines in the presence of different concentrations of a) Mg- doped NiO and b) Mg-doped NiO\ MWCNTs nanocomposite

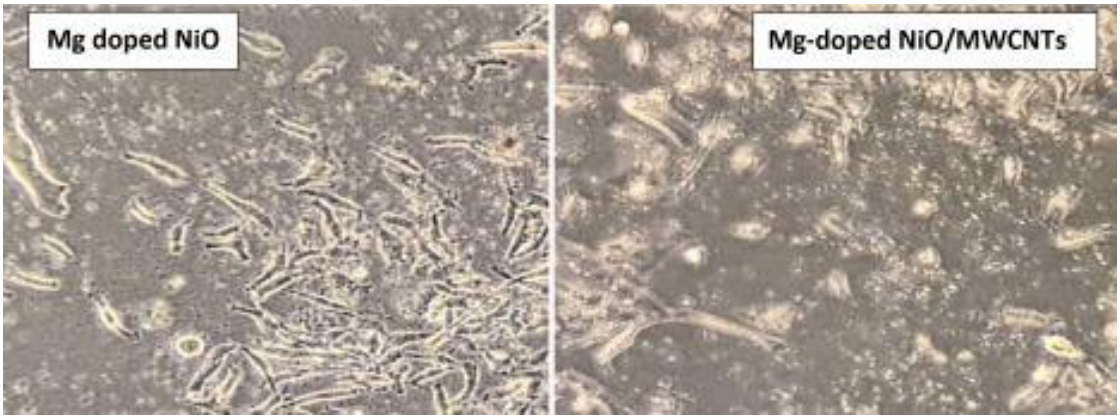

Fig. 8. The morphology of viability WRL68 cell line when treated with a) Mg-doped NiO and b) Mg-doped NiO/MWCNTs nanocomposite, after incubated 24 h

NiO/MWCNTs nanocomposites to form reactive oxygen spices (ROS), and most importantly, the apoptotic, programmed cell death, and necrotic, direct cell damage, in tumor cells populations [13]. The results also reveal capability of ROS generation of the Mg-doped NiO and Mg-doped NiO/MWCNTs nanocomposite. Besides, indicate the direct connection between the tumor cell and MWCNTs, cell type and concentrations of conjugates as demonstrate in nanocomposite.

As shown in Fig. 7, the increasing levels of ROS induce significant damage to the DNA of the cells, resulting in the arrest of cell-cycle and subsequently cell death [39, 40]. The high concentration of Mg-doped NiO might have increased the production of oxygen free radicals within the cells which causes cell death as shown in Fig. 7a. Besides, the cytotoxic effects of Mg-doped NiO/MWCNTs nanocomposites are generally resulted by the high level of (ROS) and or less Mg ions as shown in Fig. 7b. The formation of ROS results in more oxidative stress and oxidant damage in cells. The results suggested that cytotoxicity is related to release Mg- doped NiO from the extracellular degradation of nanocomposite. Cells could also phagocytize high content of Mg-doped NiO, and MWCNTs released from the intracellular degradation of nanocomposite in the acidic environment of lysosome could also induce cytotoxicity, as shown in Fig. 8 a,b which reveals the morphology of WRL68 cell line when treated with Mg-doped NiO and Mg-doped NiO\MWCNTs nanocomposites, respectively [15].

CONCLUSIONS

The Mg-doped NiO and Mg-doped NiO/MWCNTs were successfully prepared by sol-gel method. The UV-Vis sapectroscopy showed that all the prepared samples had a high absorbance and decreases the energy band gap to 2.82 eV. It was observed that the Mg-doped NiO/MWCNTs nanocomposite had good physical stability and a high zeta potential value up to - 31mV. The XRD and EDX analysis displayed that the formation of the Mg-doped NiO/MWCNTs nanocomposite, which has a cubic phase and a high crystalline nature. The FE- SEM images confirm the success of deposition of the Mg-NiO on the surface of the treated MWCNTs through the appearance of spherical shapes over the cylindrical tubes. The higher concentrations (400 pg\ml) of Mg-doped NiO and Mg-doped NiO/MWCNTs nanocomposites improved low cytotoxicity against MCF-7 and WRL68 cell lines.

CONFLICT OF INTEREST

The authors declare that there is no conflict of interests regarding the publication of this manuscript.

REFERENCE

1. Poole Jr, C.P. and F.J. Owens, Introduction to nanotechnology. 2003: John Wiley & Sons.
2. Trojanowicz M. Analytical applications of carbon nanotubes: a review. TrAC Trends in Analytical Chemistry. 2006;25(5):480-9.
3.Mirabootalebi, S.O. and G.H. Akbari, Methods for synthesis of carbon nanotubes-Review. Int. J. Bio-Inorg. Hybr.

Nanomater, 2017. 6(2): p. 49-57.
4. Ahmed DS, Abed AL. Controlled Surface Modification of CNTs using Mild Acids through Powerful Sonication Technique. Acta Physica Polonica A. 2018;134(1):7-10.
5. Ahmed DS, Haider AJ, Mohammad MR. Comparesion of Functionalization of Multi-Walled Carbon Nanotubes Treated by Oil Olive and Nitric Acid and their Characterization. Energy Procedia. 2013;36:1111-8.
6. Allaedini G, Tasirin SM, Aminayi P. Synthesis of CNTs via chemical vapor deposition of carbon dioxide as a carbon source in the presence of NiMgO. Journal of Alloys and Compounds. 2015;647:809-14.
7. Morais RG, Rey-Raap N, Costa RS, Pereira C, Guedes A, Figueiredo JL, et al. Hydrothermal Carbon/Carbon Nanotube Composites as Electrocatalysts for the Oxygen Reduction Reaction. Journal of Composites Science. 2020;4(1):20.
8. Zhao T, Ji X, Jin W, Yang W, Li T. Hydrogen storage capacity of single-walled carbon nanotube prepared by a modified arc discharge. Fullerenes, Nanotubes and Carbon Nanostructures. 2017;25(6):355-8.
9. Kazeimzadeh F, Malekfar R, Houshiar M. The effect of graphitic target density on carbon nanotube synthesis by pulsed laser ablation method. Author(s); 2018.
10. Belin T, Epron F. Characterization methods of carbon nanotubes: a review. Materials Science and Engineering: B. 2005;119(2):105-18.
11. Khoshhesab ZM, Sarfaraz M. Preparation and Characterization of NiO Nanoparticles by Chemical Precipitation Method. Synthesis and Reactivity in Inorganic, Metal-Organic, and Nano-Metal Chemistry. 2010;40(9):700-3.
12. Hosny NM. Synthesis, characterization and optical band gap of NiO nanoparticles derived from anthranilic acid precursors via a thermal decomposition route. Polyhedron. 2011;30(3):470-6.
13. Vinardell MP, Mitjans M. Antitumor Activities of Metal Oxide Nanoparticles. Nanomaterials (Basel). 2015;5(2):1004-21.
14. Dineshkumar B, Krishnakumar K, Bhatt AR, Paul D, Cherian J, John A, et al. Single-walled and multi-walled carbon nanotubes based drug delivery system: Cancer therapy: A review. Indian Journal of Cancer. 2015;52(3):262.
15.Mohammad, R., Duha S. Ahmed, Mustafa KA Mohammed & Mohammad. Chem. Pap, 2020. 74: p. 197-208.
16. Allaedini G, Aminayi P, Tasirin SM. Structural properties and optical characterization of flower-like Mg doped NiO. AIP Advances. 2015;5(7):077161.
17. Mohseni Meybodi S, Hosseini SA, Rezaee M, Sadrnezhaad SK, Mohammadyani D. Synthesis of wide band gap nanocrystalline NiO powder via a sonochemical method. Ultrasonics Sonochemistry. 2012;19(4):841-5.
18. Lingaraju K, Raja Naika H, Nagabhushana H, Jayanna K, Devaraja S, Nagaraju G. Biosynthesis of Nickel oxide Nanoparticles from Euphorbia heterophylla (L.) and their biological application. Arabian Journal of Chemistry. 2020;13(3):4712-9.
19. Anand GT, Nithiyavathi R, Ramesh R, John Sundaram S, Kaviyarasu K. Structural and optical properties of nickel oxide nanoparticles: Investigation of antimicrobial applications. Surfaces and Interfaces. 2020;18:100460.
20. Budiredla N, Kumar A, Thota S, Kumar J. Synthesis and Optical Characterization of Mg1-xNixO Nanostructures. ISRN Nanomaterials. 2012;2012:1-8.
21. Bhatt AS, Bhat DK, Santosh MS, Tai C-w. Chitosan/NiO nanocomposites: a potential new dielectric material. Journal of Materials Chemistry. 2011;21(35):13490.
22.Saravanakkumar, D., et al., Structural Investigation on Synthesized Ag DopedZnO-MWCNTand Its Applications. Journal of Nano science, Nano engineering & Applications ISSN: 2231-1777 (Online), 2018. 8(2): p. 2321-5194.
23. Soomro RA, Ibupoto ZH, Sirajuddin, Abro MI, Willander M. Electrochemical sensing of glucose based on novel hedgehog-like NiO nanostructures. Sensors and Actuators B: Chemical. 2015;209:966-74.
24.Kumar, P.V., A.J. Ahamed, and A. Ravikumar, Synthesis of Mg2+ doped NiO nanoparticles and their structural and optical properties by Co-precipitation method. JOURNAL OF ADVANCED APPLIED SCIENTIFIC RESEARCH, 2020. 2(2): p. 1-9.
25.Saravanakkumar, D., et al., Synthesis of NiO doped ZnO/MWCNT Nanocomposite and its charecterization for photocatalytic & antimicrobial applications. *J. Appl. Phys, 2018. 10: p. 73-83.*
26. Karnaukhov TM, Vedyagin AA, Cherepanova SV, Rogov VA, Mishakov IV. Sol–gel synthesis and characterization of the binary Ni–Mg–O oxide system. Journal of Sol-Gel Science and Technology. 2019;92(1):208-14.
27. Mohammed MKA, Ahmed DS, Mohammad MR. Studying antimicrobial activity of carbon nanotubes decorated with metal-doped ZnO hybrid materials. Materials Research Express. 2019;6(5):055404.
28. Cheng X, Zhong J, Meng J, Yang M, Jia F, Xu Z, et al. Characterization of Multiwalled Carbon Nanotubes Dispersing in Water and Association with Biological Effects. Journal of Nanomaterials. 2011;2011:1-12.
29. Cui H, Yan X, Monasterio M, Xing F. Effects of Various Surfactants on the Dispersion of MWCNTs-OH in Aqueous Solution. Nanomaterials (Basel). 2017;7(9):262.
30. Soylu M, Dere A, Al-Sehemi AG, Al-Ghamdi AA, Yakuphanoglu F. Effect of calcination and carbon incorporation on NiO nanowires for photodiode performance. Microelectronic Engineering. 2018;202:51-9.
31. Ahmad M, Ahmed E, Hong ZL, Khalid NR, Ahmed W, Elhissi A. Graphene–Ag/ZnO nanocomposites as high performance photocatalysts under visible light irradiation. Journal of Alloys and Compounds. 2013;577:717-27.